

OBSERVATIONAL EVIDENCE FOR STRONG DISK COMPTONIZATION IN GRO J1655 – 40

Aya KUBOTA¹ and Kazuo MAKISHIMA²

aya@astro.isas.ac.jp

*Department of Physics, University of Tokyo, 7-3-1 Hongo, Bunkyo-ku,
Tokyo 113-0033, Japan*

and

Ken EBISAWA³

*code 662, Laboratory of High Energy Astrophysics, NASA/Goddard Space Flight Center,
Greenbelt, MD 20771, U.S.A*

ABSTRACT

Analysis was made of the multiple *RXTE*/PCA data on the promised black hole candidate with superluminal jet, GRO J1655 – 40, acquired during its 1996–1997 outburst. The X-ray spectra can be adequately described by the sum of an optically thick disk spectrum and a power-law. When the estimated 1–100 keV power-law luminosity exceeds 1×10^{37} erg s⁻¹ (assuming a distance of 3.2 kpc), the inner disk radius and the maximum color temperature derived from a simple accretion disk model (a multi-color disk model) vary significantly with time. These results reconfirm the previous report by Sobczak et al. (1999). In this strong power-law state (once called “very high state”), the disk luminosity decreases with temperature, in contradiction to the prediction of the standard Shakura-Sunyaev model. In the same state, the intensity of the power-law component correlates negatively with that of the disk component, and positively

¹present address: Institute of Space and Astronautical Science, 3-1-1 Yoshinodai, Sagami-hara, Kanagawa 229-8510, Japan

²Also Cosmic Radiation Laboratory, Institute of Physical and Chemical Research

³Also Universities Space Research Association

with the power-law photon index, suggesting that the strong power-law is simply the missing optically thick disk emission. One possible explanation for this behavior is inverse-Compton scattering in the disk. By re-fitting the same data incorporating a disk Comptonization, the inner radius and temperature of the underlying disk are found to become more constant. These results provide one of the first observational confirmations of the scenario of disk Comptonization in the strong power-law state. This strong power-law state seems to appear when color temperature of the disk exceeds the certain threshold, $\sim 1.2 - 1.3$ keV.

Subject headings: black hole physics

1. Introduction

When the mass accretion rate is high, a black hole binary (BHB) resides in the soft state, which is characterized by a very soft spectrum, accompanied by a power-law tail. The soft spectral component is believed to be thermal emission from an optically thick accretion disk around a central BH (e.g., Makishima et al. 1986), because it can be reproduced by a multi-color disk model (MCD model, Mitsuda et al. 1984) which approximates emission from a standard accretion disk (Shakura & Sunyaev 1973). The model has two parameters; the maximum color temperature of the disk, T_{in} , and an apparent inner radius r_{in} . Using a spectral hardening factor of $\kappa \simeq 1.7-2.0$ (Shimura & Takahara 1997), and a correction factor for the inner boundary condition, $\xi = 0.41$ (Kubota et al. 1998), r_{in} can be related to the true inner radius R_{in} , as

$$R_{\text{in}} = \kappa^2 \cdot \xi \cdot r_{\text{in}} \quad . \quad (1)$$

X-ray observations indicate that R_{in} remains constant at $6R_{\text{g}}$ that is the last stable orbit for a non-spinning BH (R_{g} is the gravitational radius).

Although this “standard picture” remained generally successful (e.g., Ebisawa et al. 1993, Tanaka & Lewin 1995), recently two deviations from its predictions have been noticed in some soft-state BHBs. One is quite small values of R_{in} , compared to $6R_{\text{g}}$, and the other is significant variations in R_{in} . The former is found in the superluminal jet sources, GRO J1655 – 40 and GRS 1915 + 105 (e.g., Zhang et al. 1997). The latter includes GRO J1655 – 40 (Sobczak et al. 1999; hereafter S99), LMC X-1 (Wilms et al. 2001) and XTE J1550 – 564 (Kubota 2001). Although these anomalies are often attributed, e.g., to strong disk Comptonization and/or very high value of κ , no convincing evidence has been available. These issues may be related to the general theoretical belief that the standard-disk picture is valid only for a rather limited range of the mass accretion rate (e.g., Esin et al. 1997).

In order to examine to what extent the standard picture is valid, we have analyzed X-ray spectra of GRO J1655 – 40 obtained by multiple pointings with *RXTE*. This BHB has been reported to exhibit the two peculiarities mentioned above. Moreover, its BH mass, distance, and inclination angle are accurately estimated to be $7.02 \pm 0.22 M_{\odot}$, 3.2 ± 0.2 kpc, and $69.5 \pm 0.08^{\circ}$, respectively (e.g., Orosz & Bailyn 1997). These make GRO J1655 – 40 ideal for our purpose.

2. Observation and data reduction

We analyzed 72 archival data sets of GRO J1655 – 40 obtained with the *RXTE*/PCA, covering the 16-months outburst in 1996–1997. This is the same dataset as utilized by S99 except for the last few observations when the source exhibited a signature of the hard state. We co-added the data from the individual proportional counter units, and produced one co-added spectrum for each pointing. We select good data in the basic manner for bright sources.

We estimated the PCA background for each observation using *pcabackest* version 2.1e. In order to correct a possible < 10 % over/under-estimation of the background by the *pcabackest*, we compared the on-source spectra and the predicted model background spectra in the hardest energy band (60–100 keV), where the signal flux is usually negligible. When necessary, we adjusted the normalization factor of the background spectrum by $-10 \sim +10\%$. We make the response matrix for each observation using *pcarsp* version 7.10, and add 1% systematic error to each energy bin of the PCA spectrum. Over the 20–35 keV range, we increased the systematic error to 10%, to take into account the response uncertainties associated with the Xe-K edge at ~ 30 keV.

3. Data analysis and results

3.1. Standard modeling

According to the canonical spectral modeling, we fit the obtained 3–30 keV PCA spectra of GRO J1655 – 40 with the MCD plus a power-law. After Yamaoka et al. (2001), we subject the MCD component to several absorption features (a line and edges). We do not discuss these absorption features any further. To the two constituent continuum components, we apply a common photoelectric absorption with the column fixed at $N_{\text{H}} = 7 \times 10^{21} \text{ cm}^{-2}$, by referring to the *ASCA*/GIS data of this source on 1997 Feb.26 (Kubota 2001). Moreover, as for the data obtained before 1996 May 21 (MJD 50224), we fix the power-law photon index

Γ 2.1, because the power-law component was too weak to constrain Γ .

The fits have been acceptable for all the PCA spectra. In Fig.1, we show evolution of the best-fit model parameters, including the disk bolometric luminosity, $L_{\text{disk}}(\equiv 4\pi\sigma r_{\text{in}}^2 T_{\text{in}}^4)$, the 1–100 keV power-law luminosity, L_{pow} , calculated assuming an isotropic emission, and their sum, L_{tot} . Thus, the entire PCA data span of this source can be divided into three characteristic periods, referring mainly to L_{pow} . The 1st period (Period 1; before day 141) is characterized by a very low level of L_{pow} , while it is very high ($> 1 \times 10^{37}$ erg s $^{-1}$) in Period 2, which was once called “very high state” by S99. In Period 3 (after the data gap), L_{pow} returns low.

In Period 3, the values of R_{in} , which are obtained by utilizing eq.(1) with $\kappa = 1.7$ and $\xi = 0.41$, remain constant (26 km) against relatively large intensity variation, while in Period 2 they are observed to change significantly between ~ 6 km and ~ 24 km. When we fix R_{in} at 26 km and instead allow N_{H} to vary, the fits for the Period 1 and 2 data become significantly worse (Fig.1e), and N_{H} changes violently. Thus, the variation of R_{in} is real as long as we utilize the canonical two components model with constant values of κ and ξ . Clearly, GRO J1655 – 40 in Period 2 violates the standard picture.

In order to highlight the anomalies of GRO J1655 – 40, we plot L_{disk} against T_{in} in Fig.2a. For comparison, we also plot the data points of a typical BHB, LMC X-3 (e.g., Kuiper et al. 1988), of which the BH mass (5–7.2 M_{\odot}) and the inclination angle (65°–69°) are both quite similar to those of GRO J1655 – 40. The results on LMC X-3 were obtained through the spectral fitting of the same PCA data as reported by Wilms et al. (2001). Thus, the data points for LMC X-3 follow a simple relation of $L_{\text{disk}} \propto T_{\text{in}}^4$ with a constant R_{in} as L_{disk} varied by a factor of 10. Moreover, assuming its distance and inclination angle as 55 kpc and 66° respectively, the absolute value of R_{in} is calculated as ~ 60 km, which coincide with $6R_{\text{g}}$ for a BH of $6M_{\odot}$. In other words, the accretion disk in LMC X-3 perfectly satisfies the standard picture. In contrast, GRO J1655 – 40 exhibits a distinct behavior on this $T_{\text{in}}-L_{\text{disk}}$ plane. The data points in Period 2 and Period 1 deviate from the standard $L_{\text{disk}} \propto T_{\text{in}}^4$ relation, while those of Period 3 satisfy the relation except that the value of R_{in} is much smaller than that of LMC X-3.

Although the deviation from the standard picture has been found in both Period 1 and 2, it is much more significant in Period 2 than in Period 1. In addition, the observed PCA spectra in Period 1 are relatively similar to those in Period 3 (see S99), while those in Period 2 are characterized by very strong hard emission component. Therefore in this letter, we mainly focussed on the anomalous behavior in Period 2. Hereafter, we call Period 2 *anomalous regime*, while call Period 3 *standard regime*.

3.2. Differences between *anomalous* and *standard* regimes

A prominent difference between the *anomalous* and *standard* regimes is found in behavior of the power-law component. In the *anomalous regime*, L_{pow} negatively correlates to L_{disk} , in such a way that L_{tot} is kept approximately constant at a ceiling value of $\sim 1.7 \times 10^{38} \text{ erg s}^{-1}$ (Fig.1a). To our surprise, this ceiling corresponds roughly to $\sim 15 \%$ of the Eddington luminosity, $L_E \sim 1.1 \times 10^{39} \text{ erg s}^{-1}$ (assuming solar abundance) for a $\sim 7M_\odot$ BH in GRO J1655 – 40, instead of L_E itself. Furthermore, as shown in Fig.3, Γ gradually increases as L_{pow} gets higher in the *anomalous regime*, while it stays constant at ~ 2.1 in the *standard regime*. Therefore, the property of the hard component in the *anomalous regime* may be intrinsically different from that in the *standard regime*.

A simple interpretation of the source behavior in the *anomalous regime* is to presume that there emerges a third spectral component, which is harder than the MCD emission but softer than the hard component in the *standard regime*. Then, the strong anti-correlation between L_{pow} and L_{disk} , seen in the *anomalous regime*, can be explained by assuming that this third component strongly and negatively correlates with the MCD component. It is therefore natural to assume that some fraction of the photons emitted from the optically thick accretion disk are converted into the third spectral component, instead of directly reaching us. The third component is most probably produced through inverse-Compton scattering of the MCD photons by high energy electrons that may reside around the disk.

3.3. Spectral fitting incorporating a Comptonized component

We re-fit the same PCA spectra in the *anomalous regime*, with a three-component model, obtained by adding a Comptonized blackbody (“*compbb*”; Nishimura, Mitsuda, & Itoh 1986) component to the original two component model. The *compbb* model has four parameters; blackbody temperature T_{bb} , electron temperature T_e , Compton optical depth τ , and radiative area of the blackbody for an isotropic emission. However, we cannot constrain all these additional parameters, since the previous two-component model has given acceptable fits. We accordingly tie T_{bb} to T_{in} , assuming the seed photons for the inverse-Compton to be supplied by the optically thick accretion disk. We fix Γ of the original power-law component to 2.1, an average in the *standard regime* (Fig.3). Furthermore, to avoid a strong coupling between τ and T_e , we fix T_e at a representative value of 10 keV, considering that strong Compton cooling by ample seed soft photons from the optically-thick disk will make T_e significantly lower than in the hard state ($T_e \sim 30\text{--}50 \text{ keV}$; e.g., Grove et al. 1998).

In Fig.1c, we plot the re-estimated T_{in} with open circles. By considering the *compbb*

component, the highly deviated data points in terms of T_{in} have thus settled back to a smooth long-term trend. We also re-estimate the luminosity in Fig.2b as $L_{\text{disk}} + L_{\text{cbb}}$, where L_{cbb} is the estimated 0.1–100 keV *compbb* luminosity, assuming an isotropic emission. Thus, $L_{\text{disk}} + L_{\text{cbb}}$ plotted against the revised T_{in} approximately recovers the standard $L_{\text{disk}} \propto T_{\text{in}}^4$ relation for optically-thick accretion disks. Consequently, the value of R_{in} can also be considered to remain relatively stable, even when a significant fraction of the MCD photons is Comptonized. We conclude that some part of the power-law seen in the *anomalous regime* has the origin in the MCD photons, modified through the inverse-Compton process, and that the violent variations in the MCD parameters, on time scales of few days or shorter, is not real but apparent.

Figure 4a shows the typical PCA spectrum of GRO J1655 – 40 in the *anomalous regime*, which corresponds to Observation A (1996 Aug. 6; day 218) presented in Fig.1a, fitted with the three-component model. We also show the result from the previous two-component fit in Fig.4b, where the best-fit model is obtained in the range of 3–30 keV. although the spectrum is shown in 3–50 keV.

4. Discussion

In §3, we have shown that the scenario of the strong disk Comptonization successfully explains the *anomalous regime* of GRO J1655 – 40, and that the underlying disk really satisfies the standard picture. A very similar phenomenon has been observed in another Galactic jet source, XTE J1550 – 564 (Kubota 2001). Although the disk Comptonization has been discussed extensively in the literature, our results provide one of the first unambiguous observational confirmations of such a picture. Then, what causes such a strong Comptonization? As mentioned in §1, it was theoretically pointed out that the standard disk cannot be stable under high accretion rates. The *anomalous regime* can be hence considered to occur when the accretion rate reaches a certain upper critical level, as indicated by the location of *anomalous regime* (upper right) in Fig.2b.

We however remember that the critical disk luminosity, at which the *anomalous* behavior of GRO J1655 – 40 appears, is only $\sim 15\%$ of L_{E} , and that LMC X-3 exhibits no such deviation from the standard-disk even with L_{disk} close to L_{E} . Another important difference between these two BHs is that the value of R_{in} for GRO J1655 – 40 is only $\sim 2R_{\text{g}}$ for a $7M_{\odot}$ BH even in the *standard regime*, while that of LMC X-3 agrees with $6R_{\text{g}}$. This fact makes the values of T_{in} for GRO J1655 – 40 much higher than those for LMC X-3 when compared at the similar luminosity. Interestingly, the observed value of the temperature of GRO J1655 – 40, ~ 1.2 keV, which corresponds to the critical luminosity, is almost the same

as the upper limit of T_{in} (~ 1.3 keV) for LMC X-3. We hence suggest that the endpoint of the *standard regime* is not determined by the luminosity but instead by the temperature, which is thought to be ~ 1.2 – 1.3 keV for both LMC X-3 and GRO J1655 – 40. Such a consideration is consistent with a theoretical expectation that, at a high temperature, the opacity of the disk is given by electron scattering instead of photo-electric absorption that dominates at lower temperatures.

Thus, we consider that the systematically higher T_{in} (or smaller R_{in}) is responsible for the anomalous behavior of GRO J1655 – 40. Because the innermost stable orbit becomes smaller for a prograde rotation around a spinning BH, down to $\sim R_{\text{g}}$ in the extreme case, the anomalous behavior of GRO J1655 – 40 may be attributed ultimately to its BH spin, as already suggested by Zhang et al. (1997), and Makishima et al. (2000).

We would like to thank Prof. H. Inoue and Prof. S. Mineshige for helpful discussions. We are also grateful to Dr. C. Done for valuable comments and discussions.

REFERENCES

- Ebisawa, K., Makino, F., Mitsuda, K., Belloni, T., Cowley, A., Schmidke, P., & Treves, A. 1993, ApJ, 403, 684
- Esin, A., McClintock, J.E., & Narayan, R. 1997, ApJ, 489, 865
- Grove et al. 1998, ApJ, 500, 899
- Kubota, A., 2001, Ph.D. Thesis, University of Tokyo
- Kubota, A., Tanaka, Y., Makishima, K., Ueda, Y., Dotani, T., Inoue, H., & Yamaoka, K. 1998, PASJ, 50, 667
- Kuiper, L., van Paradijs, J., & van der Klis, M. 1988, A & A, 203, 79
- Makishima, K., et al. 1986, ApJ, 308, 635
- Makishima, K., et al. 2000, ApJ, 535, 632
- Mitsuda, K., et al. 1984, PASJ, 36, 741
- Nishimura, J., Mitsuda, K., & Itoh, M. 1986, PASJ, 38, 819
- Orosz, J.A. & Bailyn C.D. 1997, ApJ, 477, 876
- Shakura, N.I., & Sunyaev, R.A. 1973, A&A, 24, 337
- Shimura, T. & Takahara F. 1995, ApJ 445, 780
- Sobczak, G.J., McClintock, J.E., Remillard, R.A., Bailyn, C.D. & Orosz J.A. 1999, ApJ 520, 776 (S99)
- Tanaka, Y., & Lewin, W.H.G. 1995, in X-ray Binaries, ed. W.H.G. Lewin, J. van paradijs, & W.P.J. van den Heuvel (Cambridge University Press, Cambridge), 126

Wilms, J. et al. 2001, MNRAS, 320, 327

Yamaoka, K., Ueda, Y., Inoue, H., Nagase, F., Ebisawa, K., Kotani, T., Tanaka, Y., & Zhang, S.N. 2001, PASJ, 53, 179

Zhang, S.N., Cui, W., & Chen, W. 1997, ApJ, 482, L155

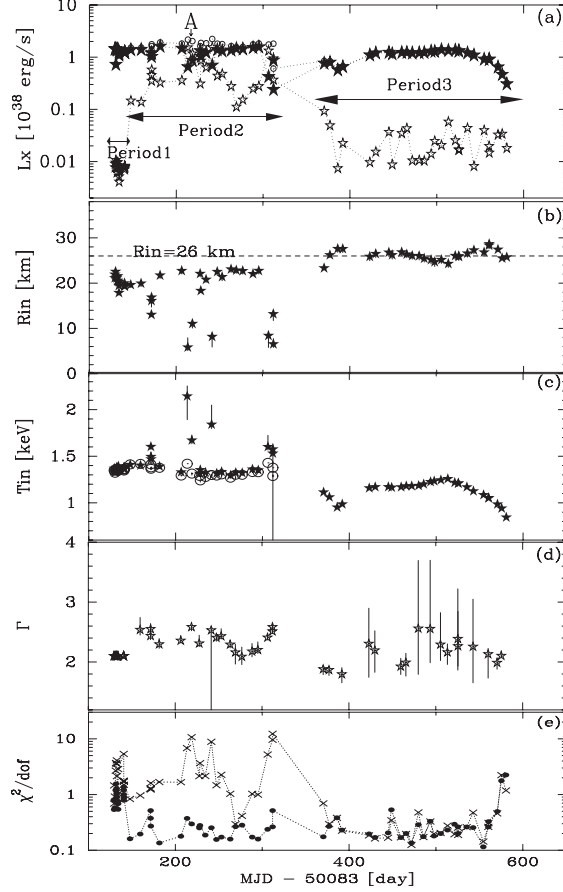


Fig. 1.— Long-term variation of the spectral parameters of GRO J1655 – 40. (a) Histories of L_{disk} (filled star), L_{pow} (open star), and L_{tot} (open circle), The three characteristic periods are indicated in the top panel. (b)–(d) Time histories of r_{in} , T_{in} , and Γ , respectively. Large circles in panel (c) represent T_{in} obtained by incorporating the disk-Comptonization. (e) That of χ^2/dof ; filled circles represent χ^2/dof with the free- R_{in} and fixed- N_{H} fits, whereas crosses those when R_{in} is fixed at 26 km and N_{H} is left free.

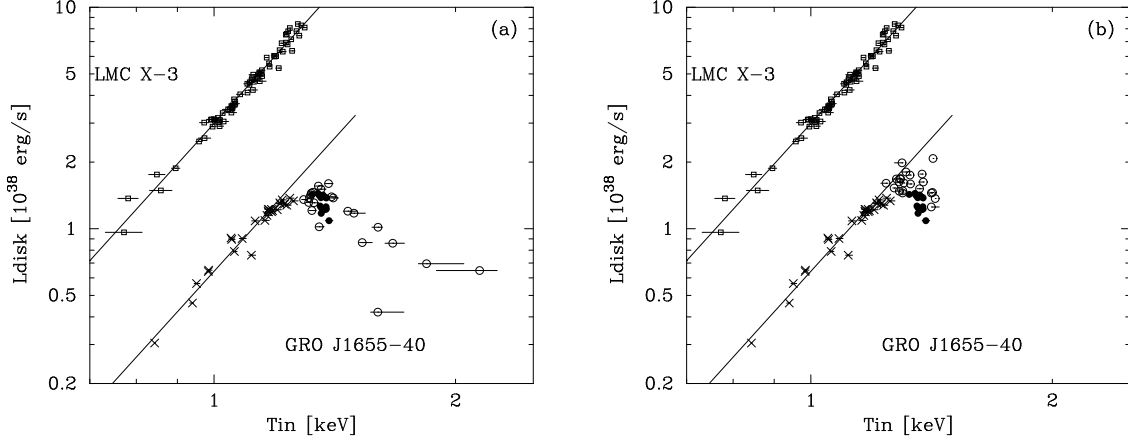


Fig. 2.— (a) The calculated L_{disk} plotted against the observed T_{in} . As for GRO J1655 – 40, three kinds of symbols specify the data obtained during Period 1 (filled circles), Period 2 (open circles), and Period 3 (crosses). The results of LMC X-3 (open squares) are also plotted for comparison. The solid lines represent the $L_{\text{disk}} \propto T_{\text{in}}^4$ relation. (b) Same as in panel (a), but the data points in Period 2 (*anomalous regime*) of GRO J1655 – 40 are re-calculated considering the Comptonized component as $L_{\text{disk}} + L_{\text{cbb}}$.

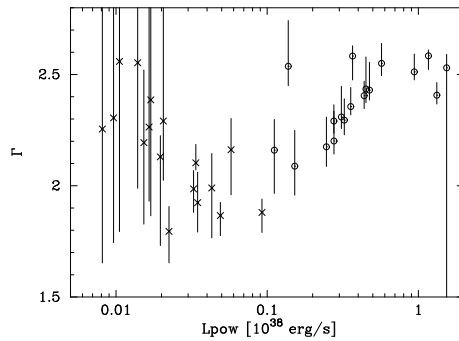


Fig. 3.— The observed Γ plotted against L_{pow} . Symbols are the same as in Fig.2.

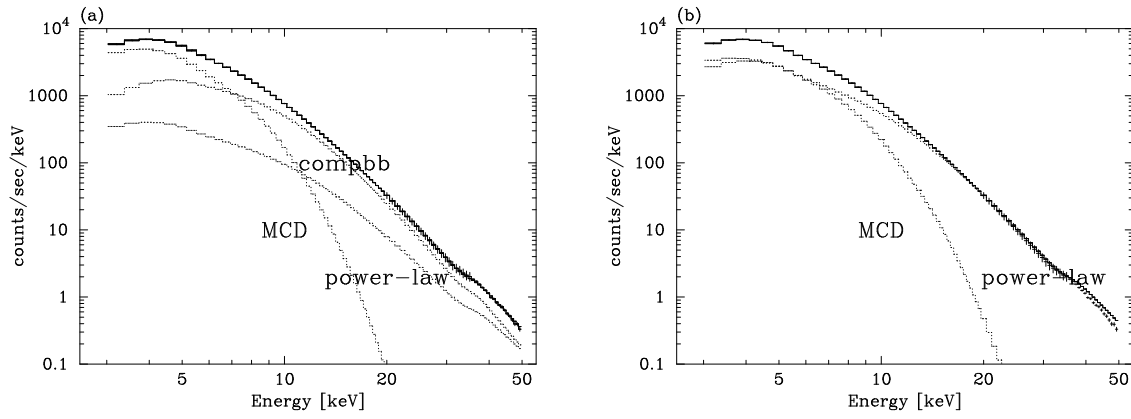


Fig. 4.— The PCA spectrum of GRO J1655 – 40 obtained in Observation A in Fig.1a. Predictions of the best-fit three-component model (panel a) and the canonical two-component model (panel b) are also shown, together with individual components.